Research on Engineering Structures & Materials
journal homepage: http://www.jresm.org
Research Group

*Research Article*

# Analytical evaluation of plasticity models for anisotropic materials with experimental validation

Emre Esener*[a], Aysema Ünlü[b]

*Department of Mechanical Engineering, Bilecik Seyh Edebali University, Bilecik, Turkey*

**Article Info**

*Article history:*
Received 26 Oct 2021
Revised 11 Dec 2021
Accepted 17 Dec 2021

*Keywords:*

*Plasticity modeling;*
*Anisotropy;*
*Aluminum alloy;*
*TBF1050*

**Abstract**

The plastic behavior of a material can be represented by plasticity models. The ability of plasticity models to represent material behavior depends on their mathematical form, the assumptions they hold, and the sensitivity of the input parameters. Plasticity models are of great importance, especially in finite element analysis. While the mathematical forms of plasticity models are implemented in finite element analysis software, some coding-related inaccuracies may occur. Therefore, the capacity of the plasticity model to represent the plastic behavior of the material can be revealed more accurately by examining it analytically. After this verification, the choice of the plasticity model to be used in the finite element analysis can be realized with more accuracy and less time loss. In this direction, in this study, the capacity of plasticity models, which are frequently used today, to model the plastic behavior of anisotropic materials was evaluated. For this purpose, Hill48, Barlat89, Hu2003 and Poly6 plasticity models were analyzed analytically and TBF1050 3rd generation advanced high strength steel and 5XXX series aluminum alloy were used as materials. The predictive capacities of the plasticity models were evaluated with the yield locus and angular variations of anisotropy coefficient and yield stress ratios. As a result, it has been revealed that polynomial-based models can model the plasticity behavior of the material more accurately for both material groups.



## 1. Introduction

In order to model the plastic deformations that occur in the material in plastic forming methods, the determination of material models that describe the elastic and plastic behavior of the material is very critical in terms of method engineering. In this context, it is equally important to accurately determine the necessary material parameters for material models. Plastic behavior is a more complex concept than elastic behavior of materials. In the elastic part, there is a linear relationship between strains and stresses by means of Hooke's law. In general, plastic strains are not defined by stresses alone. Plastic strains depend on the entire loading history and how the stress state is reached [1]. During a plastic forming process, the materials exhibit non-linear behavior due to hardening. In order to model the plastic behavior of a material under general stress condition, a yield criterion describing the relationship between stress components at the time of yielding, a yield rule describing the relationship between stress and strain ratio components, and a hardening rule describing the evolution of the initial yield stress during the deformation process is needed. The yield criteria (plasticity models) which describe the plastic behavior of materials determined by mathematical models. Yield criteria contain a margin of error due to their constructs, containing assumptions, or number of input parameters. This margin of error in the yield criteria, greatly affects the prediction accuracy of material

*Corresponding author: emre.esener@bilecik.edu.tr
[a] orcid.org/0000-0001-5854-4834; [b] orcid.org/0000-0002-4288-6212
DOI: http://dx.doi.org/10.17515/resm2021.356me1026

behavior. Predictions performed in this way show low accuracy and have time-consuming steps. In industrial applications engineers generally uses well-known plasticity models to describe the plastic behavior of materials. These models show significantly poor performance, especially on new generation materials. For this reason, engineers in the industry, generally analyze the material behavior by using different plasticity models based on the trial-and-error method. This procedure continues until a plasticity model predicts the material behavior within the expected tolerance of the product. The analyzes of material behavior performed in this way are time-consuming and this causes major problems especially for mass production. The choice of yield criterion is of great importance at this point. Simple experimental verifications are made in order to give the effective result of the selected yield criterion. Among the mechanical tests, tensile test, fatigue test, shear test, and hydraulic bulge test are the most frequently used tests for experimental verification. If the yield criteria are validated by experimental data, the above-mentioned time and cost loss will be less in the design stage of the process.

There are many yield criteria in the literature [2-7]. These criteria, which define the material behavior, contain various assumptions according to the material and hardening conditions. Models can be divided into two categories according to the isotropic and anisotropic behavior assumptions of the material. Isotropy is a concept related to uniformity and states that the properties of the material will not change with different crystallographic orientations, that is, they will be independent of the direction. The concept of anisotropy, on the other hand, states that the mechanical properties may change depending on the direction due to the crystal structure of the material or the characteristics of the rolling process. The direction-dependent change in plastic behavior with anisotropy is expressed by the term called Lankford parameter or anisotropy coefficient [8]. This parameter can be determined by a uniaxial tensile test. Anisotropy values are usually determined by displacement measurements taken after 20% elongation from the tensile test. In the literature, it is generally performed for three different directions (rolling direction, diagonal direction, transverse direction) [9-11].

With the help of the yield criteria, yield loci of materials are obtained and the behavior of the material under loading conditions is determined with these surfaces. Yield loci should be closed, convex and smooth. Stresses within the surface line cause elastic deformation, while stresses above the surface line cause plastic deformation. Stresses outside the locus have no physical meaning. While the horizontal axis represents the rolling direction, the vertical axis represents the 90º direction (transverse) to the rolling direction. With the help of yield criteria, directional yield stress ratios and anisotropy coefficients can also be predicted. Sensitivity of the yield criterion prediction can be validated by experimental data. Analytical verification of plasticity models before finite element analysis prevents time loss in process design. Otherwise, a finite element analysis should be performed at each trial stage in order to determine the plasticity model that yields sensitive results. While obtaining the yield loci of a model takes a short time, a complex form of non-linear finite element analysis takes hours. As explained above, in the finite element analysis step of production methods, it is very important to determine the yield criterion that makes an accurate and precise prediction.

Material grade can affect the plasticity model predictions since the material behavior varies with the material grade. For the automotive industry, materials with low thickness, high strength, good formability, shock absorbing ability, collision resistance and low cost are of great importance to ensure safety without sacrificing lightness [12]. In this context, Advanced High Strength Steels (AHSS) are used in the automotive industry. New generation AHSSs are handled in three generations according to their technological developments [12]. Third generation AHSSs were produced due to the strength capabilities of the first-generation steels were limited and the second-generation steels

were expensive hence they contained high-cost alloying elements [13]. These steels are materials with high formability and high strength and at the same time produced with lower costs. Today, third generation AHSSs are increasingly being incorporated into automotive production to increase vehicle fuel efficiency and crash resistance [14]. In this context, three steel classes called TBF (TRIP Aided Bainitic Ferrite) steels, QP (Quenching & Partitioning) steels and Nano steels have been developed as the third generation AHSSs [15]. Among the third generation improved high strength steels, TBF steels stand out due to their properties such as high ductility, formability, toughness, fatigue strength and delayed fracture strength.

Aluminum alloys, on the other hand, are industrial materials that are widely used in applications that require advanced technology. Here, automobiles, aircraft and ship industries are the most important areas of use. Aluminum and its alloys are generally called light alloys and their strength is increased by adding different alloying elements to the base material (aluminum), which is ductile and has high corrosion resistance. Unlike iron-based materials, they contain small amounts of alloying elements. The main alloying element of aluminum 5XXX alloys is magnesium [16]. They are known for their general strength, corrosion resistance and weldability. The tensile strength increases with increasing magnesium ratio [17]. These series alloys are mostly used in marine transportation vehicles and automotive industry.

The aim of the study is to analyze the analytical models of yield criteria based on their predictive performance of the plastic behavior of the anisotropic materials. In this direction, analytical performance evaluations of yield criteria for steel and non-ferrous materials actively used in the automotive industry were performed and the evaluations were confirmed by mechanical tests.

## 2. Materials and Method

In this study, cold-rolled Aluminum 5XXX alloy and cold-rolled TBF1050 steel with gauge thickness values as 1.5 mm and 1.2 mm, respectively are used. TBF (TRIP-assisted baintic-ferritic) steels are in use as 3rd generation of advanced high strength steels (AHSS). In this study, TBF-grades with a minimum tensile strength of 1050 MPa is used. The high strength of these steel stems from a fine-grained martensitic or bainitic matrix while an increased fraction of retained austenitic inclusions utilize the TRIP effect which leads to enhanced elongations [18-19]. TBF1050 steel used in this study is not subjected any heating stage. In the aluminum alloy that is used in this study, the main alloying element is magnesium and strain hardening grade of aluminum alloy is H1.

### 2.1. Material Testing

In the first stage of the study, uniaxial tensile tests were performed to obtain the verification parameters. Tensile tests were performed in ASTM-E8 standard [20] and with 3 repetitions. Uniaxial tensile tests were carried out on the 300 kN capacity Zwick/Roell Z300E testing machine and the dimensional changes in length and width of the specimens were measured with extensometers. Anisotropy coefficients and yield stress ratios were obtained as a result of the tests with a strain rate of 0.0067 1/s performed in 7 directions ($0^o$, $15^o$, $30^o$, $45^o$, $60^o$, $75^o$, $90^o$).

In the second step of the study, hydraulic bulge tests were performed to obtain biaxial anisotropy coefficient and biaxial yield stress ratios. Hydraulic bulge tests were carried out in 3 repetitions on a 600 kN capacity Zwick/Roell BUP600 test device using 200x200 mm square specimens. In hydraulic bulge tests, strain values were obtained using the GOM Argus system with the Digital Image Correlation (DIC) method by non-contact cameras. In these tests, biaxial yield stresses were obtained by using linear fit region to stress-strain

curve of the materials in addition biaxial anisotropy coefficients were calculated with the ratio of the strains. Strain values are obtained by DIC method.

The visuals of the mechanical tests are given in Fig. 1. Anisotropy coefficients and yield stress ratios obtained from the mechanical tests are shown in Table 1.

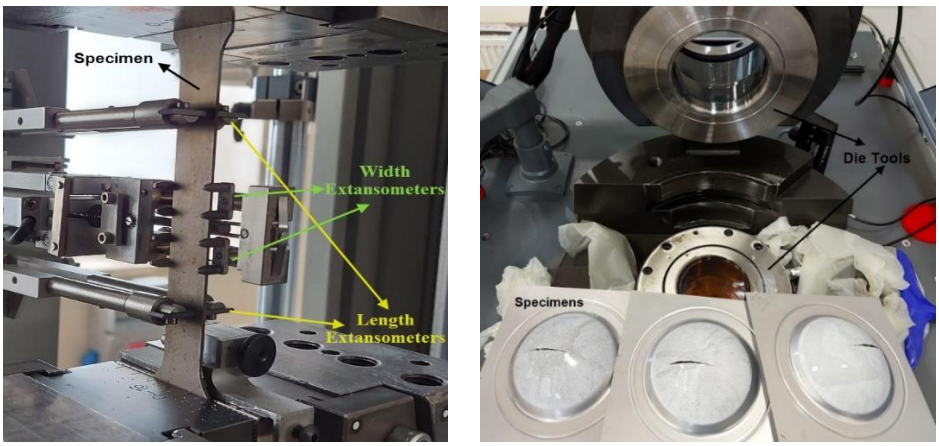


(a) (b)

Fig. 1 Mechanical test systems (a) Uniaxial tensile test (b) Hydrolic bulge test

As it can be seen from the Fig. 1. Uniaxial tensile tests were performed with length and width extensometers. The elongation in the length of the test sample and the contraction in the width of the test sample are measured with these extensometers. The changes by means of the material gauge thickness are obtained by the volume constancy. Anisotropy coefficients (r) are calculated by using ratio of the strain values as given in the Eq. (1).

$$r = \frac{\varepsilon_w}{\varepsilon_t} \tag{1}$$

where, $\varepsilon_w$ is the width strain and $\varepsilon_t$ is the thickness strain.

Table 1. Material validation parameters obtained with mechanical tests

| Material | | Angle (°) | | | | | | | Biaxial |
|---|---|---|---|---|---|---|---|---|---|
| | | 0 | 15 | 30 | 45 | 60 | 75 | 90 | |
| TBF1050 | Anisotropy coefficent | 0.95 | 0.93 | 1.08 | 1.06 | 0.99 | 1.04 | 1.10 | 0.98 |
| | Yield stress ratio | 1 | 1.03 | 1.04 | 1.04 | 1.04 | 1.03 | 1.05 | 0.97 |
| AA5XXX | Anisotropy coefficent | 0.80 | 0.74 | 0.71 | 0.71 | 0.75 | 0.80 | 0.81 | 1.01 |
| | Yield stress ratio | 1 | 0.99 | 0.99 | 0.99 | 0.99 | 1.01 | 0.99 | 1.11 |

### 2.2. Plasticity Models

In this study, Hill48, Barlat89, Hu2003 and 6th order polynomial based (Poly6) plasticity models were used to model the plastic behavior of anisotropic materials. In this part of the study, the analytical expressions of the plasticity models are explained. The first yield

criterion for anisotropic materials was presented by R. Hill in 1948 [21] and this quadratic criterion is given in the Eq. (2).

$$2f = F\left(\sigma_{yy} - \sigma_{zz}\right)^2 + G(\sigma_{zz} - \sigma_{xx})^2 + H\left(\sigma_{xx} - \sigma_{yy}\right)^2 + 2L{\tau_{yz}}^2 + 2M{\tau_{zx}}^2 + 2N{\tau_{xy}}^2 = 1 \quad (2)$$

In the equation above, F, G, H, L, M and N are the material parameters to be calibrated. For plane stress condition, this criterion can be expresses as,

$$22f = (G + H)\sigma_{sx}^2 - 2H\sigma_{xx}\sigma_{yy} + (F + H)\sigma_{yy}^2 + 2N\sigma_{xy}^2 = 1 \quad (3)$$

These parameters were determined based on Lankford's coefficients using Eqs. (4)-(7) This situation is named as "Hill48-r based" within the scope of the study.

$$F = \frac{r_0}{r_{90}(1+r_0)} \quad (4)$$

$$G = \frac{1}{1 + r_0} \quad (5)$$

$$H = \frac{r_0}{1+r_0} \quad (6)$$

$$N = \frac{(r_0 + r_{90})(1 + 2r_{45})}{2r_{90}(1 + r_0)} \quad (7)$$

Here, $r_0$, $r_{45}$ and $r_{90}$ represent the anisotropy coefficients in the rolling direction, 45 degrees to the rolling direction and 90 degrees to the rolling direction, respectively. Due to the simple r-based approach of the Hill48 criterion in defining the anisotropies of materials, it offers a great advantage to the users, and this advantage makes this criterion still one of the most frequently used criteria today [22-24]. F, G, H and N coefficients can also be calculated on the basis of stress in the Hill48 yield criterion. This situation is named as "Hill48-Stress (S) based" within the scope of the study. Stress-based expressions of these parameters are given in Eqs. (8)-(11).

$$F = \frac{1}{2}\left(\left(\frac{\sigma_0}{\sigma_{90}}\right)^2 - 1 + \left(\frac{\sigma_0}{\sigma_b}\right)^2\right) \quad (8)$$

$$G = \frac{1}{2}\left(1 - \left(\frac{\sigma_0}{\sigma_{90}}\right)^2 + \left(\frac{\sigma_0}{\sigma_b}\right)^2\right) \quad (9)$$

$$H = \frac{1}{2}\left(1 + \left(\frac{\sigma_0}{\sigma_{90}}\right)^2 - \left(\frac{\sigma_0}{\sigma_b}\right)^2\right) \quad (10)$$

$$N = \frac{1}{2}\left(\left(\frac{2\sigma_0}{\sigma_{45}}\right)^2 - \left(\frac{\sigma_0}{\sigma_b}\right)^2\right) \quad (11)$$

where $\sigma_b$ represents the biaxial yield stress.

In 1989, Barlat and Lian presented a criterion for materials with planar anisotropy under plane stress conditions [25]. This criteron allows the use of the Lankford parameters for the definition of the anisotropy. Barlat89 criterion can be written as Eq. (12).

$$f = a|k_1 + k_2|^M + a|k_1 - k_2|^M + c|2k_2|^M = 2\sigma_e^M \quad (12)$$

Here "M" exponent depends on the crystal structure of materials. For face centered cubic (FCC) materials M = 8 is recommended and for body centered cubic (BCC) materials M = 6 may be used [26]. $k_1$ and $k_2$ coefficients can be written as Eq. (13) and (14).

$$k_1 = \frac{\sigma_{11} + h\sigma_{22}}{2} \quad (13)$$

$$k_2 = \left[\left(\frac{\sigma_{11}-h\sigma_{22}}{2}\right)^2 + p^2\sigma_{12}^2\right]^{1/2} \quad (14)$$

a, c, and h represent material constants are obtained through $r_0$, $r_{45}$, and $r_{90}$. These parameters can be written as Eqs. (15-17).

$$a = 2 - 2\sqrt{\left(\frac{r_0}{1+r_0}\right)\left(\frac{r_{90}}{1+r_{90}}\right)} \quad (15)$$

$$c = 2 - a \quad (16)$$

$$h = \sqrt{\left(\frac{r_0}{1+r_0}\right)\left(\frac{1+r_{90}}{r_{90}}\right)} \quad (17)$$

"p" parameter can be found by optimization. Barlat89 model is one of the most used models in finite element analyses since the model has a simple construction and needs a few numbers of material parameters [27-29].

Hu, developed the Hill48 criterion in 2003 and proposed a new plasticity model [30]. The Hu-2003 criterion can be written in the general form as in Eq. (18).

$$f(\overline{\sigma}) = \frac{1}{\sigma_0^4}\sigma_1^4 - \frac{4r_0}{(1+r_0)\sigma_0^4}\sigma_1^3\sigma_2 + \left(\frac{1}{\sigma_b^4} - \frac{1}{\sigma_0^4} - \frac{1}{\sigma_{90}^4} + \frac{4r_0}{(1+r_0)\sigma_0^4} + \frac{4r_{90}}{(1+r_{90})\sigma_{90}^4}\right)\sigma_1^2\sigma_2^2 - \frac{4r_{90}}{(1+r_{90})\sigma_{90}^4}\sigma_1\sigma_2^3 + \frac{1}{\sigma_{90}^4}\sigma_2^4 + \left(\frac{16}{(1+r_{45})\sigma_{45}^4} - \frac{2}{\sigma_b^4}\right)(\sigma_1^2 + \sigma_2^2 - \sigma_1\sigma_2)\sigma_{12}^2 + \left(\frac{1}{\sigma_b^4} + \frac{16r_{45}}{(1+r_{45})\sigma_{45}^4}\right)\sigma_{12}^4 = 1 \quad (18)$$

According to this criterion, it has the ability to model the plastic behavior of the material with a total number of 7 parameters: anisotropy coefficients in the rolling direction, 45 degrees to the rolling direction and 90 degrees to the rolling direction, yield stresses in the same directions and hydraulic bulge test yield stress.

The sixth-order homogeneous polynomial yield criterion (Poly6) was developed by Soare in order to describe anisotropic behavior of materials [31]. Poly6 criterion could be used for not only plane stress but also 3D stress state. Besides, the derivatives of polynomial functions could easily be computed and this provides convenience for implementation of the material model into finite element (FE) codes. The model has 16 material coefficients for plane stress state and it can be expressed as follows:

$$f = a_1{\sigma_x}^6 + a_2{\sigma_x}^5\sigma_y + a_3{\sigma_x}^4{\sigma_y}^2 + a_4{\sigma_x}^3{\sigma_y}^3 + a_5{\sigma_x}^2{\sigma_y}^4 + a_6\sigma_x{\sigma_y}^5 + a_7{\sigma_y}^6 + \left(a_8{\sigma_x}^4 + a_9{\sigma_x}^3\sigma_y + a_{10}{\sigma_x}^2{\sigma_y}^2 + a_{11}\sigma_x{\sigma_y}^3 + a_{12}{\sigma_y}^4\right){\sigma_{xy}}^2 + \left(a_{13}{\sigma_x}^2 + a_{14}\sigma_x\sigma_y + a_{15}{\sigma_y}^2\right){\sigma_{xy}}^4 + a_{16}{\sigma_{xy}}^6 \quad (19)$$

Qui et.al. [32] developed an analytical determination of anisotropic parameters for Poly6 yield criterion. The parameters of Poly6 yield criterion are expressed with the r-values and yield stresses without any optimization method. According to their study $a_1$-$a_7$ parameters can be calculated analytically using the Eqs. (20)-(26).

$$a_1 = 1 \quad (20)$$

$$a_7 = \left(\frac{\sigma_0}{\sigma_{90}}\right)^6 \quad (21)$$

$$a_2 = -6\frac{r_0}{r_0+1} \quad (22)$$

$$a_6 = -6\frac{r_{90}}{r_{90}+1}a_7 \tag{23}$$

$$a_5 = \frac{3}{2}\frac{r_b-1}{r_b+1}\left(\frac{\sigma_0}{\sigma_b}\right)^6 + \frac{1}{4}\left[\left(\frac{\sigma_0}{\sigma_b}\right)^6 + \left(\frac{\sigma_0}{\sigma_\tau}\right)^6\right] - [(a_6 + 2a_7) - (a_1 + a_2)] \tag{24}$$

$$a_3 = \frac{1}{2}\left[\left(\frac{\sigma_0}{\sigma_b}\right)^6 + \left(\frac{\sigma_0}{\sigma_\tau}\right)^6\right] - (a_1 + a_5 + a_7) \tag{25}$$

$$a_4 = \left(\frac{\sigma_0}{\sigma_b}\right)^6 - (a_1 + a_2 + a_3 + a_5 + a_6 + a_7) \tag{26}$$

In Ref. [32] $\sigma_\tau$ is calculated from the analytical Poly4 [31] and given in Eq. (27).

$$\frac{\sigma_0}{\sigma_\tau} = \left\{\left(\frac{\sigma_0}{\sigma_b}\right)^4 + 8\left[\frac{r_0}{r_0+1} + \frac{r_{90}}{r_{90}+1}\left(\frac{\sigma_0}{\sigma_{90}}\right)^4\right]\right\}^{1/4} \tag{27}$$

Then $a_{16}$ coefficient is expressed as Eq. (28)

$$a_{16} = \left\{16[1 - (r_{45}+1)^{-1}]\left(\frac{\sigma_0}{\sigma_{45}}\right)^4 + \left(\frac{\sigma_0}{\sigma_b}\right)^4\right\}^{3/2} \tag{28}$$

Other eight parameters ($a_8$ - $a_{15}$) is determined from the uniaxial tension test.

$$Y_1(\theta)a_8 + Y_2(\theta)a_9 + Y_3(\theta)a_{10} + Y_4(\theta)a_{11} + Y_5(\theta)a_{12} + Y_6(\theta)a_{13} + Y_7(\theta)a_{14} + Y_8(\theta)a_{15} = \Gamma_y(\theta) \tag{29}$$

where

$$Y_1(\theta) = cos^{10}\theta\, sin^2\theta \tag{30}$$

$$Y_2(\theta) = cos^8\theta\, sin^4\theta \tag{31}$$

$$Y_3(\theta) = cos^6\theta\, sin^6\theta \tag{32}$$

$$Y_4(\theta) = cos^4\theta\, sin^8\theta \tag{33}$$

$$Y_5(\theta) = cos^2\theta\, sin^{10}\theta \tag{34}$$

$$Y_6(\theta) = cos^8\theta\, sin^4\theta \tag{35}$$

$$Y_7(\theta) = cos^6\theta\, sin^6\theta \tag{36}$$

$$Y_8(\theta) = cos^4\theta\, sin^8\theta \tag{37}$$

$$\Gamma_y(\theta) = \left(\frac{\sigma_0}{\sigma_\theta}\right)^6 - z_y(\theta) - cos^6\theta\, sin^6\theta\, a_{16} \tag{38}$$

$$z_y(\theta) = a_1\, cos^{12}\theta + a_2\, cos^{10}\theta\, sin^2\theta + a_3\, cos^8\theta\, sin^4\theta + a_4\, cos^6\theta\, sin^6\theta + a_5\, cos^4\theta\, sin^8\theta + a_6\, cos^2\theta\, sin^{10}\theta + a_7\, sin^{12}\theta \tag{39}$$

Based on the definition of r$\theta$ Eq. (40) can be written.

$$R_1(\theta)a_8 + R_2(\theta)a_9 + R_3(\theta)a_{10} + R_4(\theta)a_{11} + R_5(\theta)a_{12} + R_6(\theta)a_{13} + R_7(\theta)a_{14} + R_8(\theta)a_{15} = \Gamma_r(\theta) \tag{40}$$

where,

$$R_1(\theta) = \left[r_p(\theta)cos^2\theta - 4\right]cos^8\theta\, sin^2\theta \tag{41}$$

$$R_2(\theta) = \left[r_p(\theta)cos^2\theta\, sin^2\theta - (1 + 2\, sin^2\theta)\right]cos^6\theta\, sin^2\theta \tag{42}$$

$$R_3(\theta) = \left[r_p(\theta)cos^2\,\theta\,sin^2\,\theta - 2\right] cos^4\,\theta\,sin^4\,\theta \tag{43}$$

$$R_4(\theta) = \left[r_p(\theta)cos^2\,\theta\,sin^2\,\theta - (1 + 2\,cos^2\,\theta)\right] cos^2\,\theta\,sin^6\,\theta \tag{44}$$

$$R_5(\theta) = \left[r_p(\theta)sin^2\,\theta - 4\right] cos^2\,\theta\,sin^8\,\theta \tag{45}$$

$$R_6(\theta) = \left[r_p(\theta)cos^2\,\theta - 2\right] cos^6\,\theta\,sin^4\,\theta \tag{46}$$

$$R_7(\theta) = \left[r_p(\theta)cos^2\,\theta\,sin^2\,\theta - 1\right] cos^4\,\theta\,sin^4\,\theta \tag{47}$$

$$R_8(\theta) = \left[r_p(\theta)sin^2\,\theta - 2\right] cos^4\,\theta\,sin^6\,\theta \tag{48}$$

$$\Gamma_r(\theta) = z_r(\theta) - z_y(\theta)r_p(\theta) - r_p(\theta)cos^6\,\theta\,sin^6\,\theta\,a_{16} \tag{49}$$

$$r_p(\theta) = \frac{6}{r_\theta + 1} \tag{50}$$

$$\begin{aligned} z_r(\theta) = {} & (6a_1 + a_2)cos^{10}\,\theta + (5a_2 + 2a_3)cos^8\,\theta\,sin^2\,\theta + \\ & (4a_3 + 3a_4)cos^6\,\theta\,sin^4\,\theta + (3a_4 + 4a_5)cos^4\,\theta\,sin^6\,\theta + \\ & (2a_5 + 5a_6)cos^2\,\theta\,sin^8\,\theta + (a_6 + 6a_7)\,sin^{10}\,\theta \end{aligned} \tag{51}$$

As Eqs. (29) and (40) are the linear equations of $a_8$-$a_{15}$, the parameters can be analytically solved with eight equations. If five r-values and three uniaxial tension yield stresses are used, the expressions of $a_8$-$a_{15}$ can be calculated as Eq. (52) and this situation is named as "r-based Poly6" in this study. If three r-values and five UT (uniaxial tension) yield stresses are used the expressions of $a_8$-$a_{15}$ can be calculated as Eq. (53) and this situation is named as "Stress(S)-based Poly6" in this study.

$$\begin{bmatrix} a_8 \\ a_9 \\ a_{10} \\ a_{11} \\ a_{12} \\ a_{13} \\ a_{14} \\ a_{15} \end{bmatrix} = \begin{bmatrix} R_1(\theta_1) & R_2(\theta_1) & R_3(\theta_1) & R_4(\theta_1) & R_5(\theta_1) & R_6(\theta_1) & R_7(\theta_1) & R_8(\theta_1) \\ R_1(\theta_2) & R_2(\theta_2) & R_3(\theta_2) & R_4(\theta_2) & R_5(\theta_2) & R_6(\theta_2) & R_7(\theta_2) & R_8(\theta_2) \\ R_1(\theta_3) & R_2(\theta_3) & R_3(\theta_3) & R_4(\theta_3) & R_5(\theta_3) & R_6(\theta_3) & R_7(\theta_3) & R_8(\theta_3) \\ R_1(\theta_4) & R_2(\theta_4) & R_3(\theta_4) & R_4(\theta_4) & R_5(\theta_4) & R_6(\theta_4) & R_7(\theta_4) & R_8(\theta_4) \\ R_1(\theta_5) & R_2(\theta_5) & R_3(\theta_5) & R_4(\theta_5) & R_5(\theta_5) & R_6(\theta_5) & R_7(\theta_5) & R_8(\theta_5) \\ Y_1(\theta_6) & Y_2(\theta_6) & Y_3(\theta_6) & Y_4(\theta_6) & Y_5(\theta_6) & Y_6(\theta_6) & Y_7(\theta_6) & Y_8(\theta_6) \\ Y_1(\theta_7) & Y_2(\theta_7) & Y_3(\theta_7) & Y_4(\theta_7) & Y_5(\theta_7) & Y_6(\theta_7) & Y_7(\theta_7) & Y_8(\theta_7) \\ Y_1(\theta_8) & Y_2(\theta_8) & Y_3(\theta_8) & Y_4(\theta_8) & Y_5(\theta_8) & Y_6(\theta_8) & Y_7(\theta_8) & Y_8(\theta_8) \end{bmatrix}^{-1} \begin{bmatrix} \Gamma_r(\theta_1) \\ \Gamma_r(\theta_2) \\ \Gamma_r(\theta_3) \\ \Gamma_r(\theta_4) \\ \Gamma_r(\theta_5) \\ \Gamma_y(\theta_6) \\ \Gamma_y(\theta_7) \\ \Gamma_y(\theta_8) \end{bmatrix} \tag{52}$$

$$\begin{bmatrix} a_8 \\ a_9 \\ a_{10} \\ a_{11} \\ a_{12} \\ a_{13} \\ a_{14} \\ a_{15} \end{bmatrix} = \begin{bmatrix} R_1(\theta_1) & R_2(\theta_1) & R_3(\theta_1) & R_4(\theta_1) & R_5(\theta_1) & R_6(\theta_1) & R_7(\theta_1) & R_8(\theta_1) \\ R_1(\theta_2) & R_2(\theta_2) & R_3(\theta_2) & R_4(\theta_2) & R_5(\theta_2) & R_6(\theta_2) & R_7(\theta_2) & R_8(\theta_2) \\ R_1(\theta_3) & R_2(\theta_3) & R_3(\theta_3) & R_4(\theta_3) & R_5(\theta_3) & R_6(\theta_3) & R_7(\theta_3) & R_8(\theta_3) \\ Y_1(\theta_4) & Y_2(\theta_4) & Y_3(\theta_4) & Y_4(\theta_4) & Y_5(\theta_4) & Y_6(\theta_4) & Y_7(\theta_4) & Y_8(\theta_4) \\ Y_1(\theta_5) & Y_2(\theta_5) & Y_3(\theta_5) & Y_4(\theta_5) & Y_5(\theta_5) & Y_6(\theta_5) & Y_7(\theta_5) & Y_8(\theta_5) \\ Y_1(\theta_6) & Y_2(\theta_6) & Y_3(\theta_6) & Y_4(\theta_6) & Y_5(\theta_6) & Y_6(\theta_6) & Y_7(\theta_6) & Y_8(\theta_6) \\ Y_1(\theta_7) & Y_2(\theta_7) & Y_3(\theta_7) & Y_4(\theta_7) & Y_5(\theta_7) & Y_6(\theta_7) & Y_7(\theta_7) & Y_8(\theta_7) \\ Y_1(\theta_8) & Y_2(\theta_8) & Y_3(\theta_8) & Y_4(\theta_8) & Y_5(\theta_8) & Y_6(\theta_8) & Y_7(\theta_8) & Y_8(\theta_8) \end{bmatrix}^{-1} \begin{bmatrix} \Gamma_r(\theta_1) \\ \Gamma_r(\theta_2) \\ \Gamma_r(\theta_3) \\ \Gamma_y(\theta_4) \\ \Gamma_y(\theta_5) \\ \Gamma_y(\theta_6) \\ \Gamma_y(\theta_7) \\ \Gamma_y(\theta_8) \end{bmatrix} \tag{53}$$

Using the analytical expressions of all plasticity models described above, the representativeness of the plasticity models for anisotropic materials was evaluated.

## 3. Results and Discussion

In this part of the study, the plasticity models described in Chapter 2 were analyzed analytically and converted to Matlab codes, and the directionality of anisotropy coefficients and yield stress ratios were estimated for TBF1050 and AA5XXX. The results obtained

were compared with the validation parameters obtained from mechanical tests. First, yield loci of the materials were analyzed, and the loci obtained by analytical expressions of plasticity models were compared for TBF1050 steel and AA5XXX alloy in Fig. 2 and Fig. 3, respectively.

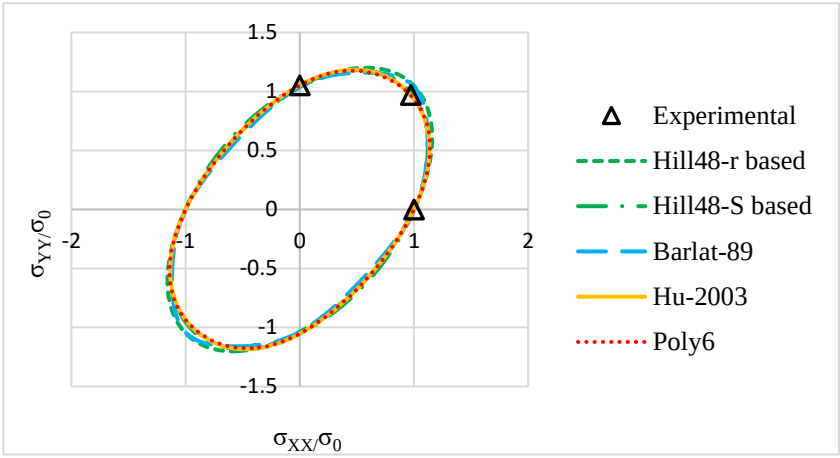


Fig. 2 Yield locus comparison for TBF1050 steel

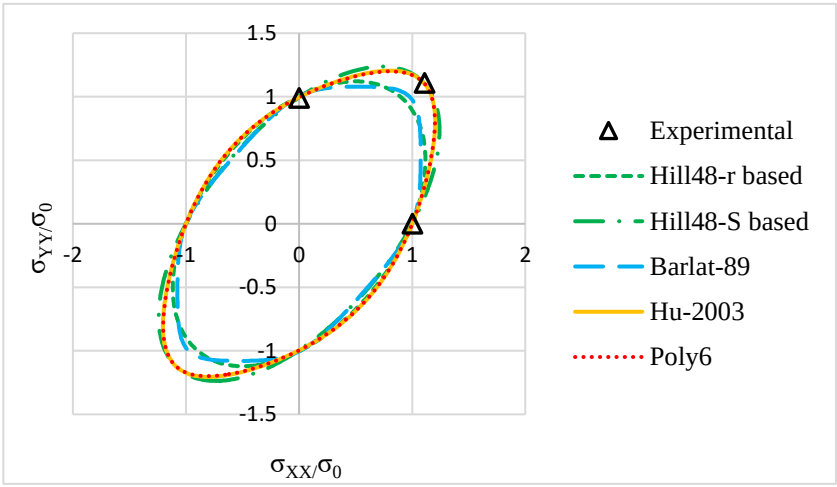


Fig. 3 Yield locus comparison for AA5XXX alloy

As it can be seen from the figures, the stress-based Hill48 model, Hu2003 model and Poly6 model for both materials represented the experimental data quite successfully and gave the most sensitive results in terms of yield loci. The Hill48-r based and Barlat89 models, on the other hand, gave close results to each other, but failed to represent the biaxial tensile behavior especially for aluminum alloy. These results shows that the stress-based of the plasticity models predicts the yield loci more accurately since the yield loci is a stress-based surface. Poly6 and Hu2003 models use the biaxial yield stress values as an input for this reason biaxial part of the yield loci can be predicted more accurately.

In the next step of the study, directional anisotropy coefficients and yield stress ratios predicted by the plasticity models were obtained. The prediction results were verified with experimental data and are shown in Figure 4-7. As can be seen from the figures, the Poly6

model for both materials gave results that are in good agreement with the experimental data. Here, the anisotropy coefficient-based version of the Poly6 model was able to model the directionality of the anisotropy coefficient values, while the stress-based version was able to model the angular variation of the yield stress ratio values exactly overlapping with the experimental data. Except for the Poly6 model, the most suitable results with the experimental data were obtained with the Hu2003 model. The Hu2003 model is in agreement with the experimental results for TBF1050 steel, except for the 30° prediction of the anisotropy coefficient and the 75° direction of the yield stress ratio estimation. However, for the AA5XXX alloy, except for the 0°, 45° and 90° directions, it predicts far from the experimental data. The stress-based version of the Hill48 model showed a successful performance in the yield stress ratio estimations of 0°, 45° and 90° directions for both materials, but showed a very poor estimation performance in the anisotropy coefficient predictions. Finally, Hill48 and Barlat89 models based on anisotropy coefficients, although giving consistent results with each other, were not successful in representing the directional material behavior, especially in terms of yield stress ratio.

These results shows that the Hill48 model (both r-based and S-based) can only predicts the rolling, diagonal, and transverse direction values since the Hill48 model use these values as input. In addition, this model shows a poor performance except these directions for both material. Barlat89 model has a similar approach with the Hill48-r based model. It can be seen from the results that the predictions of anisotropy coefficients and yield stress ratios are very similar with the Hill48-r based model. When it comes to Hu2003 model, this model can predict anisotropy coefficient directionality better than the stress ratio results since this model predominantly based on anisotropy coefficients. However, Poly6 plasticity model shows the best prediction performance for both anisotropy coefficients and stress ratio directionalities for all materials. This results shows that the increasing number of the coefficients of the plasticity models increases the prediction accuracy. Poly6 model has 16 coefficients for determining the material behavior at plane stress state. Stress based Poly6 model predicted the stress ratio values, and r-based Poly6 model predicted the anisotropy coefficients values for 7 directions with an accurate agreement with the experimental results.

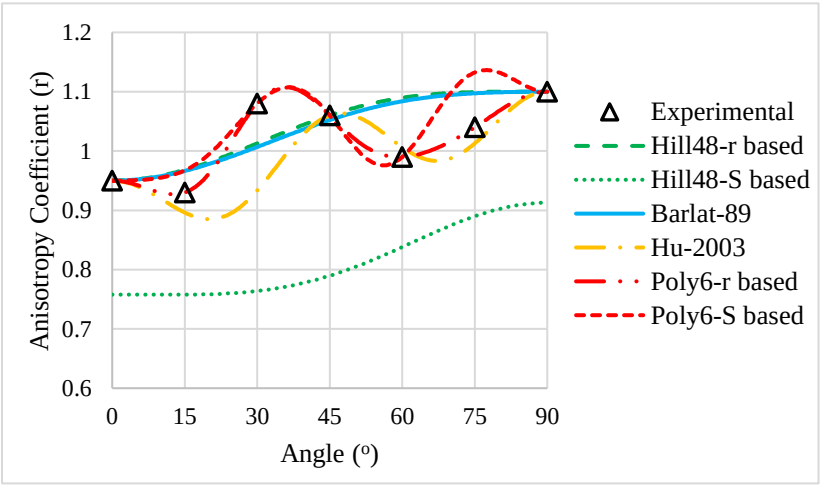


Fig. 4 Angular variation of anisotropy coefficients for TBF1050 steel

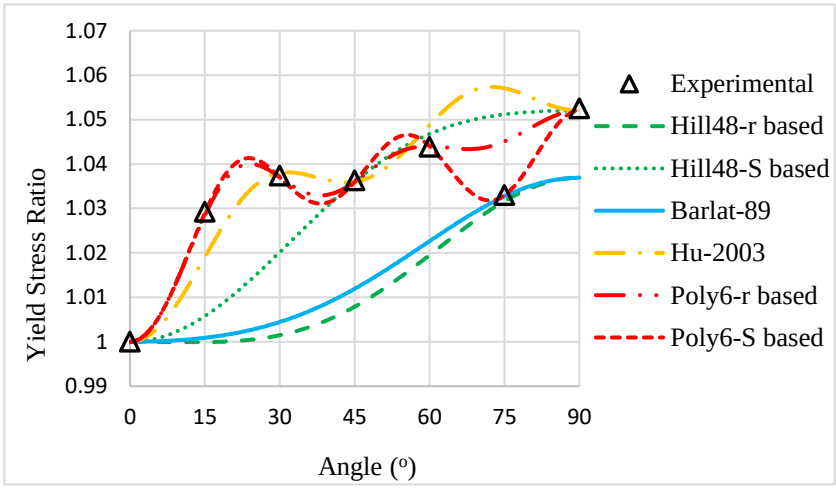


Fig. 5 Angular variation of yield stress ratios for TBF1050 steel

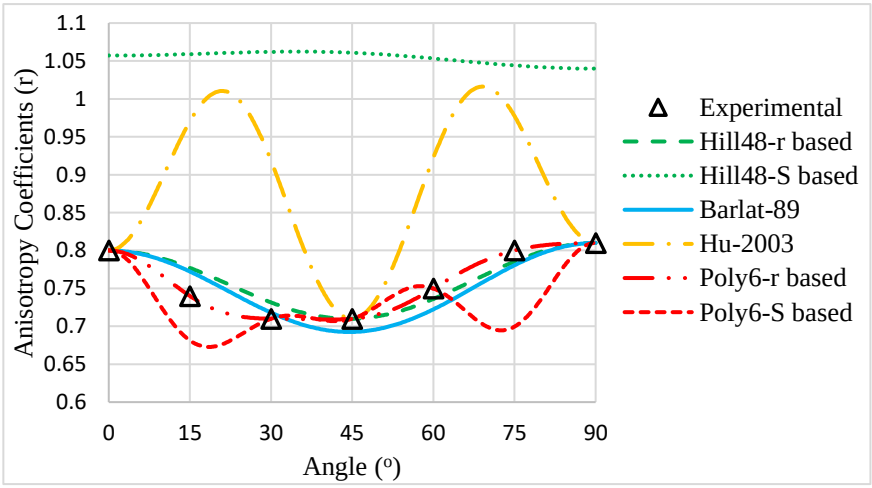


Fig. 6 Angular variation of anisotropy coefficients for AA5XXX alloy

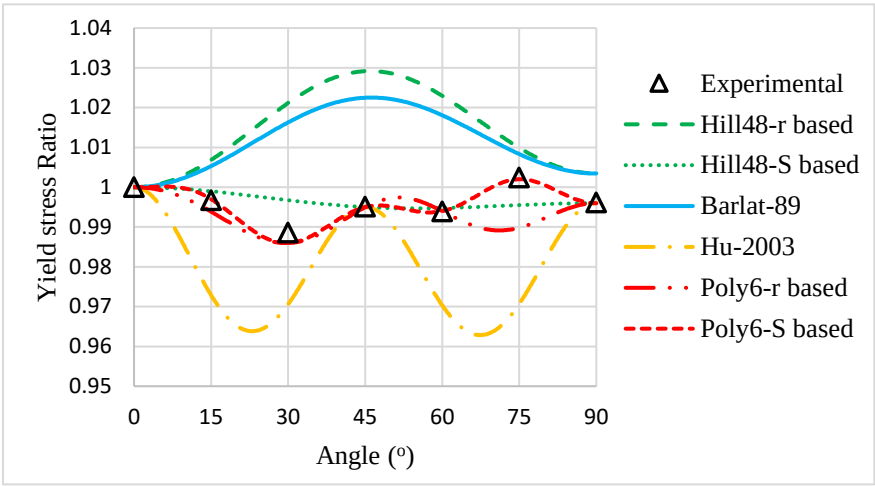


Fig. 7 Angular variation of yield stress ratios for AA5XXX alloy

## 4. Conclusions

The main purpose of the study is to model the plastic behavior of steel and non-ferrous materials by using analytical expressions of plasticity models that are frequently used today. For this purpose, the directional anisotropy coefficients and yield stress ratios of the materials were predicted by plasticity models and the prediction results were compared with the experimental data. Hill48, Barlat89, Hu2003 and Poly6 yield criteria were used as plasticity models. Among these models, Hill48 and Poly6 plasticity models were evaluated with two different versions as anisotropy coefficient-based and stress-based. Experimental data were obtained from uniaxial tensile tests performed in 7 directions (0º, 15º, 30º, 45º, 60º, 75º, 90º) and hydraulic bulge tests in order to validate the analytical models. In the study, TBF1050 steel, one of the 3rd generation advanced high strength steels, and 5XXX series aluminum alloy were used as non-ferrous material. As a result of the study, the following conclusions were reached:

- The stress-based Hill48 model, Hu2003 model and Poly6 model for both materials represented the experimental data quite successfully and performed the most sensitive results in terms of yield loci.
- The Hill48-r based and Barlat89 models presented similar behavior but failed to represent the biaxial tensile behavior especially for aluminum alloy by means of yield loci.
- The Poly6 model for both materials gave results that are in good agreement with the experimental data with the perspective of directional anisotropy coefficients and yield stress ratios.
- The anisotropy coefficient-based version of the Poly6 model was able to model the directionality of the anisotropy coefficient values, while the stress-based version was able to model the angular variation of the yield stress ratio values exactly overlapping with the experimental data.
- The Hu2003 model has an agreement with the experimental results for TBF1050 steel, except for the 30º prediction of the anisotropy coefficient and the 75º direction of the yield stress ratio estimation. However, for the AA5XXX alloy, except for the 0º, 45º and 90º directions, it predicts far from the experimental data.

- The stress-based version of the Hill48 model showed a successful performance in the yield stress ratio estimations of 0º, 45º and 90º directions for both materials, but showed a poor prediction performance in the anisotropy coefficient predictions.
- The Hill48 and the Barlat89 models based on anisotropy coefficients, although giving consistent results with each other, were not successful in representing the directional material behavior, especially in terms of yield stress ratio.

As can be seen, the most successful results were obtained with polynomial-based plasticity models. As a result of the study, it has been revealed that the plastic behavior of the materials can be modeled quite successfully with the uniaxial tensile test and hydraulic bulge test data. With an accurate finite element implementation, the plasticity models used analytically in this study can also be used in numerical studies, effectively.

## Acknowledgement

This study was supported by Bilecik Seyh Edebali University Scientific Research Projects Commission (Project Number: 2020-01.BŞEÜ.03-05, 2021).

## References

[1] Clausing DP. Effect of plastic strain state on ductility and toughness. International Journal of Fracture Mechanics, 1970; 6(1): 71-85. https://doi.org/10.1007/BF00183662

[2] Karafillis AP, Boyce MC. A general anisotropic yield criterion using bounds and a transformation weighting tensor. Journal of the Mechanics and Physics of Solids, 1993; 41(12): 1859-1886. https://doi.org/10.1016/0022-5096(93)90073-O

[3] Hill R. A user-friendly theory of orthotropic plasticity in sheet metals. International Journal of Mechanical Sciences, 1993; 35(1): 19-25. https://doi.org/10.1016/0020-7403(93)90061-X

[4] Yoshida F, Hamasaki H, Uemori T. A user-friendly 3D yield function to describe anisotropy of steel sheets. International Journal of Plasticity, 2013; 45: 119-139. https://doi.org/10.1016/j.ijplas.2013.01.010

[5] Barlat F, Brem JC, Yoon JW, et. al., Chung K, Dick RE, Lege DJ, Pourboghrat F, Choi SH, Chu E. Plane stress yield function for aluminum alloy sheets-part 1: theory. International Journal of Plasticity, 2003; 19(9): 1297-131. https://doi.org/10.1016/S0749-6419(02)00019-0

[6] Cazacu O, Plunkett B, Barlat F. Orthotropic yield criterion for hexagonal closed packed metals. International Journal of Plasticity, 2006; 22(7): 1171-1194. https://doi.org/10.1016/j.ijplas.2005.06.001

[7] Yoshida F, Uemori T. A model of large-strain cyclic plasticity describing the Bauschinger effect and workhardening stagnation. International journal of plasticity, 2002; 18(5-6): 661-686. https://doi.org/10.1016/S0749-6419(01)00050-X

[8] Banabic D, Bunge HJ, Pohlandt K, Tekkaya AE. Formability of Metallic Materials (Springer, Heidelberg, 2000). https://doi.org/10.1007/978-3-662-04013-3

[9] Wang L, Lee TC. The Effect of Yield Criteria on The Forming Limit Curve Prediction and The Deep Drawing Process Simulation. International Journal of Machine Tools & Manufacture, 2006; 46: 988-995. https://doi.org/10.1016/j.ijmachtools.2005.07.050

[10] Ozsoy M, Esener E, Ercan S, Fırat M. Springback predictions of a dual-phase steel considering elasticity evolution in stamping process. Arabian Journal for Science and Engineering, 2014; 39(4): 3199-3207. https://doi.org/10.1007/s13369-013-0910-9

[11] Banabic D. Sheet Metal Forming Processes-Constitutive Modelling and Numerical Simulation (Springer, NewYork, 2010) https://doi.org/10.1007/978-3-540-88113-1

[12] Cornette D, Cugy P, Hildenbrand A, et. al., Bouzekri M, Lovato G. Ultra high strength FeMn TWIP steels for automotive safety parts. Metallurgical Research & Technology, 2005; 102(12): 905-918. https://doi.org/10.1051/metal:2005151
[13] Billur E, Karabulut S, Yılmaz İÖ, et. al., Erzincanoğlu S, Çelik H, Altınok E, Başer T. Mechanical Properties of Trip Aided Bainitic Ferrite (TBF) Steels in Production and Service Conditions. Hittite Journal of Science and Engineering, 2018; 5(3): 231-237. https://doi.org/10.17350/HJSE19030000100
[14] Bhattacharya D, Cho L, Van der Aa E, et. al., Pichler A, Pottore N, Ghassemi-Armaki H, Findley KO, Speer JG. Influence of the Starting Microstructure of an Advanced High Strength Steel on the Characteristics of Zn-Assisted Liquid Metal Embrittlement. Materials Science &Engineering A, 2020; 804: 1-14. https://doi.org/10.1016/j.msea.2020.140391
[15] Galdos L, Argandoña ES de, Mendiguren J, et. al., Gil I, Ulibarri U, Mugarra E. Numerical simulation of U-Drawing test of Fortiform 1050 steel using different material models. Procedia Engineering, 2017; 207: 137-142. https://doi.org/10.1016/j.proeng.2017.10.751
[16] Tzeng YC, Chen RY, Lee SL. Nondestructive tests on the effect of Mg content on the corrosion and mechanical properties of 5000 series aluminum alloys. Materials Chemistry and Physics, 2021; 259: 124202. https://doi.org/10.1016/j.matchemphys.2020.124202
[17] Rana RS, Purohit R, Das S. Reviews on the influences of alloying elements on the microstructure and mechanical properties of aluminum alloys and aluminum alloy composites. International Journal of Scientific and research publications, 2012; 2(6): 1-7.
[18] Hausmann K, Krizan D, Pichler A, Werner E. TRIP-aided bainitic-ferritic sheet steel: A critical assessment of alloy design and heat treatment. Material Science and Technology (MS&T), 2013; 13: 209-218.
[19] Winkelhofer F, Hebesberger T, Krizan D, Avakemian A, Pichler A. Development of cold rolled TBF-steels with a tensile strength of 1180 MPa. voestalpine Stahl GmbH, White Paper.
[20] Standard, A.S.T.M. E8/E8M. Standard test methods for tension testing of metallic materials, 2011; 3: 66.
[21] Hill R. A theory of the yielding and plastic flow of anisotropic metals. Proceedings of the Royal Society of London. Series A. Mathematical and Physical Sciences, 1948; 193(1033): 281-297. https://doi.org/10.1098/rspa.1948.0045
[22] Wang L, Lee TC. The effect of yield criteria on the forming limit curve prediction and the deep drawing process simulation. International Journal of Machine Tools and Manufacture, 2006; 46(9): 988-995. https://doi.org/10.1016/j.ijmachtools.2005.07.050
[23] Lazarescu L, Ciobanu I, Nicodim IP, et. al., Comsa DS, Banabic D. Effect of the mechanical parameters used as input data in the yield criteria on the accuracy of the finite element simulation of sheet metal forming processes. In Key Engineering Materials, 2013; 554: 204-209. Trans Tech Publications Ltd. https://doi.org/10.4028/www.scientific.net/KEM.554-557.204
[24] Neto DM, Oliveira MC, Alves JL, Menezes LF. Influence of the plastic anisotropy modelling in the reverse deep drawing process simulation. Materials & Design, 2014; 60: 368-379. https://doi.org/10.1016/j.matdes.2014.04.008
[25] Barlat F, Lian K. Plastic behavior and stretchability of sheet metals. Part I: A yield function for orthotropic sheets under plane stress conditions. International journal of plasticity, 1989; 5(1): 51-66. https://doi.org/10.1016/0749-6419(89)90019-3
[26] Ls-Dyna Theoretical Manual. Livermore Software Technology Corporation, 1998.

[27] Liu H, Liu Y. Cross section deformation of heterogeneous rectangular welded tube in rotary draw bending considering different yield criteria. Journal of Manufacturing Processes, 2021; 61: 303-310. https://doi.org/10.1016/j.jmapro.2020.11.015
[28] Pandre S, Takalkar P, Morchhale A, et. al., Kotkunde N, Singh SK. Prediction capability of anisotropic yielding behaviour for DP590 steel at elevated temperatures. Advances in Materials and Processing Technologies, 2020; 6(2): 396-404. https://doi.org/10.1080/2374068X.2020.1728647
[29] Harpell ET, Worswick MJ, Finn M, et. al., Jain M, Martin P. Numerical prediction of the limiting draw ratio for aluminum alloy sheet. Journal of Materials Processing Technology, 2000; 100(1-3): 131-141. https://doi.org/10.1016/S0924-0136(99)00468-9
[30] Hu W. Characterized behaviors and corresponding yield criterion of anisotropic sheet metals. Materials Science and Engineering: A, 2003; 345(1-2): 139-144. https://doi.org/10.1016/S0921-5093(02)00453-7
[31] Soare S, Yoon JW, Cazacu O. On the use of homogeneous polynomials to develop anisotropic yield functions with applications to sheet forming. International Journal of Plasticity, 2008; 24(6): 915-944. https://doi.org/10.1016/j.ijplas.2007.07.016
[32] Hu Q, Yoon JW, Stoughton TB. Analytical determination of anisotropic parameters for Poly6 yield function. International Journal of Mechanical Sciences, 2021; 201: 106467. https://doi.org/10.1016/j.ijmecsci.2021.106467